Solid Freeform Fabrication 2024: Proceedings of the 35th Annual International Solid Freeform Fabrication Symposium – An Additive Manufacturing Conference
Reviewed Paper

Predictive Modeling of Drying Process in Clay 3D Printing

Subodh C. Subedi[1] and Krishnan Suresh[1]

[1]Mechanical Engineering Department, University of Wisconsin-Madison, USA

Abstract

Clay 3D printing is a unique process involving material extrusion of soft wet clay through a print head, via slicer defined paths to create a layer-wise part. Unlike fused deposition modeling (FDM) printer, where the molten filament solidifies upon extrusion, in ceramic additive manufacturing, a slurry of clay when extruded begins losing moisture due to an exothermic reaction. The diffusion of moisture within the clay, and evaporation causes drying of the entire part. The drying process is heavily influenced by part geometry, print parameters and constituent materials. Non-uniform drying can lead to defects such as delamination, voids and cracks. This paper presents a numerical model for predicting time dependent moisture in a ceramic 3D printed part. Physical experiments are used to measure moisture content at different instances of time for geometries with varying complexities. Results of physical experiments are incorporated in the numerical models to predict spatial and temporal moisture content.

Introduction

Ceramics are inorganic, non-metallic materials that have been in use for centuries. They have been traditionally used as construction materials and cookwares. However, with advancements in material and manufacturing technologies, ceramics are found today in electronic components [1], automobiles [2], aerospace [3], and medical and surgical tools [4, 5]. Ceramics exhibit very high hardness, temperature resistance, high compressive strength, chemical non-toxicity, wear resistance and low friction, making them ideal for the above applications.

Parts made out of clay are either sculpted, mold casted, injection molded or hand-built [6]. These freshly shaped 'green parts' are finished manually to remove any surface imperfections, and then fired in the kiln at over 1200°C to convert them into dense hard ceramics. These hardened parts are then glaze fired for better surface texture, color and aesthetics. The accuracy, repeatability and reliability of these parts have been well researched, and the above processes have been perfected over some centuries now. However, conventional manufacturing processes require significant costs to fabricate complex shapes. They also require specialized tools, jigs and fixtures, expensive molds, causing significant material wastage and higher lead times for low-volume production parts.

Clay 3D Printing

Additive manufacturing, or 3D printing, has been at the forefront of advanced manufacturing with its ability to manufacture complex geometries with high precision, accuracy and minimal lead times. Multiple technologies developed for polymer or metal additive manufacturing have been modified and adapted for ceramic additive manufacturing. Based on feed-stock material and deposition techniques they can be categorized into slurry-based, powder-based and bulk solid-based [7]. There are commercial technologies for clay additive manufacturing that overcome most of the limitations of conventional ceramic manufacturing processes. These printers provide design freedom, high degree of customization, rapid prototyping and reduced material wastage, making them ideal choice for hobbyist and designers.

A schematic of a typical setup for slurry based clay 3d printing - the focus of this work - is shown in Figure 1a. It is a type of material extrusion additive manufacturing process [8] that is similar to standard Fused Deposition Modelling (FDM) / Fused Filament Fabrication (FFF) in terms of material deposition. However, unlike FFF, where a heated element melts a wire filament and extrudes it out of the nozzle, in clay additive manufacturing, a slurry of clay is extruded out which solidifies due to an exothermic reaction. The feed-stock delivery system consists of a tank that stores wet clay mixed with additives to enhance different properties of the clay. The print head and mechanical-ram work in sync, controlled by a computer. The mechanical-ram squeezes out the slurry through the tubes to the print head, and the print head deposits the clay as directed by the path defined in the g-code. The slurry is pushed out of the extruder and the clay starts solidifying as it starts loosing moisture to the surrounding. A conical vase printed using clay 3D printer is shown in Figure 1b.

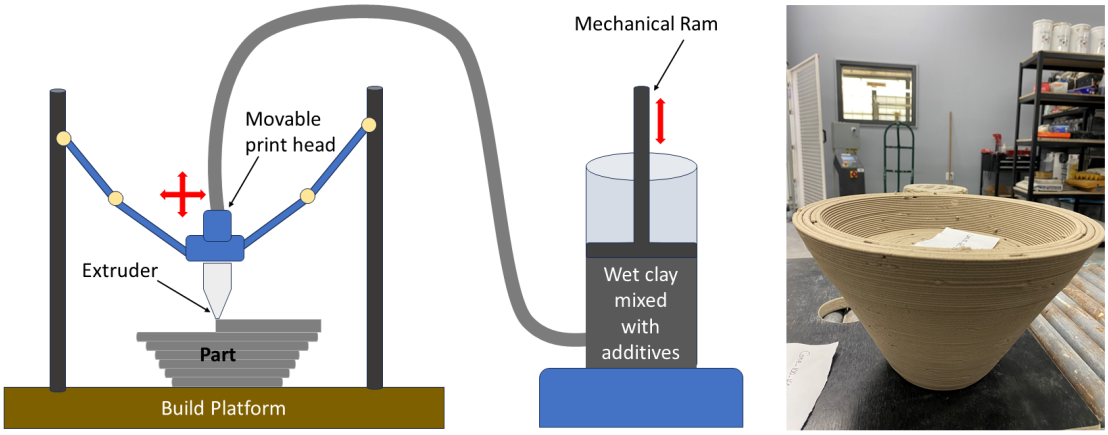

(a) *Schematic of clay 3D printer* (b) *Clay 3D printed part*

Figure 1: *Details of a Clay 3D printer.*

Failures in Clay 3D Printing

Unfortunately, there is a very high failure rate on parts printed with clay 3d printers. Part printing is a complex function of the combination of material parameters (clay density, viscosity, moisture content), process parameters (print speed, layer thickness) and geomet-

ric parameters (minimum feature size, overhang angle). As the process is adapted from polymers technology, and the material properties change significantly with time, repeatability and consistency of results in clay 3d printing is a challenging task. Indeed, successful printing required multiple attempts. Some of the common failures observed during clay additive manufacturing are shown in Figure 2. Numerous experiments and significant manual intervention is required to minimize these failures modes, and produce finished parts.

(a) *Delamination between layers.* (b) *Bulging of edges.* (c) *Separation of walls/voids.* (d) *Sagging/Collapse of thin walls.*

Figure 2: *Typical failures in clay 3D printed parts.*

These failures are primarily a result of non-uniform drying of clay. The focus of this work is on investigating the clay drying process. Drying occurs when moisture at or near the surface of clay diffuse to the surrounding through evaporation or capillary actions [9]. As the slurry of clay is exposed to air, during deposition over a build platform, it instantly initiates an exothermic reaction. It leads to loss of heat and moisture content from the slurry. This moisture causes surface tension forces to tightly pack the clay particles, causing shrinkage of layers. As additional material is added, gaps are created between adjacent surfaces. Furthermore, these tightly packed clay particles prevent the diffusion of entrapped moisture to the outer surface, leading to most of the failure modes as shown in Figure 2. Thus, a better understanding of moisture diffusion in the part can help process development and optimization of material parameters, to minimize part failures.

Most of the prior works on clay additive manufacturing involves process parameter optimization [10, 11] for enhanced functionality [12] and material strength [13, 14]. Numerous trial-and-error based physical experiments are carried out to improve process and material performance. These experiments incur significant costs and wastage of material.

There have been several investigations on concrete printing, a process similar to ceramic printing. Vantyghem et.al [15] and Ooms et.al [16] used finite element method to simulate 3D concrete printing, using multiple implicit static analyses. Every segment of tool-path was generated by adding finite elements along the path. Part failures were investigated based on maximum layer deformation obtained through numerous build analyses carried out over these finite elements added along the tool-path. Comparison between two extended FEM-based simulations were presented; however, comparison against physical experimentation was not carried out. Khan et.al [17] investigated the impact of process parameters (nozzle

diameter and printing speed) on the printability of concrete structures using similar concepts as Vantyghem [15]. Numerical simulations were carried out to identify number of layers printed until failure, defined by the deformation of layers.

Wolfs and Suiker [18] used FEM simulation and printing experiments to understand elastic buckling and plastic collapse under the dead weight of added layers of 3D printed walls made of Weber 3D 145-2 concrete mixture. Recently An et.al [19] used element tracing approach to identify layer at which part would fail due to elastic buckling or plastic collapse of walls made out of elastoplastic concrete material. Time dependent material properties were assigned to simulate thixotropic behaviour. Numerical simulations using different constitutive models provided close approximations to the analytical solutions. These numerical simulations carried out on extrusion-based additive manufacturing only examine part failures under the dead weight of the part, and neglect the effect of drying, which significantly varies these loads over time.

There are multiple software solutions available today such as Clayon [20], Wasp Clay [21], Ceramaker Printer Software [22] as well as plugins for Grasshopper [23], that slice the part to generate tool-paths for printing. Some of these tools only use the layer dead weight as structural loads and carry out static structural analysis to predict failures.

This paper proposes a simulation-driven approach to predict moisture diffusion in clay additive manufacturing, a prime reason for part failures. A customized physics-based finite element simulation tool is developed that captures the loss of moisture in a part during printing and passive-drying process. The model is validated with experimental observations for parts with varying geometric features. The overall strategy is illustrated in Figure 3.

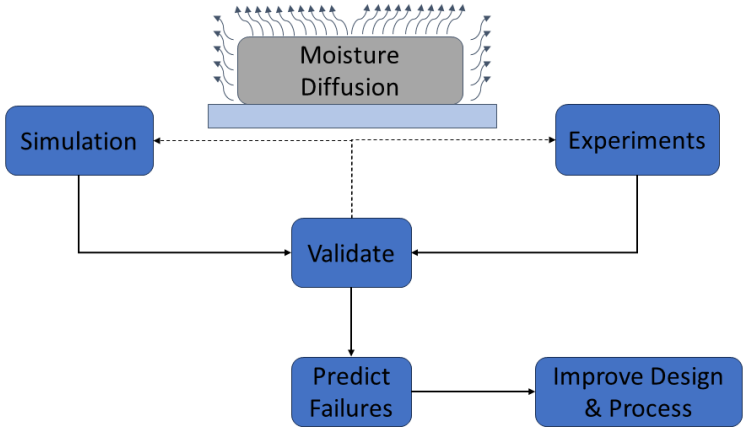

Figure 3: *Simulation and experimental validation of the drying process.*

Predictive Modeling for Moisture Diffusion

Simulating the printing process by incorporating the moisture diffusion will help qualitatively predict failures in ceramic additive manufacturing. A moisture diffusion model considers the rate of diffusion within the printed clay as well as to the atmosphere. Rate of diffusion is measured as the change in moisture content over a time period and can be

modeled using the diffusion equation (also called Fick's Law [24]):

$$\frac{\partial m}{\partial t} = D(\frac{\partial^2 m}{\partial x^2} + \frac{\partial^2 m}{\partial y^2} + \frac{\partial^2 m}{\partial z^2}) \tag{1}$$

where m is the moisture content (kg/kg) and D is the diffusion coefficient (m^2/s). The material properties of clay are dependent on moisture and rate of diffusion from the parts. These values can be obtained from physical experimentation and will require model calibration for better prediction accuracy. Data for material properties, rate of diffusion, and print conditions are required to obtain qualitative prediction of time dependent moisture contents in a part. Material properties such as density and diffusivity are considered to be constant throughout the process, whereas modulus of elasticity is defined as a function of the moisture content that decreases over time, given by,

$$E = E_0 e^{-\beta m} \tag{2}$$

where, E_0 is the initial modulus of elasticity, β is the proportionality constant and m is the moisture content.

Application Interface

A GUI-based Clay Printing Simulator (CPS) was developed incorporating the diffusion model. The Windows-based software uses 3D finite element models to simulate the moisture diffusion in clay additive manufacturing process. The software reads two files, a .STL model for the part and a g-code file for the printing process, generated using a slicing software such as Cura®. After the g-code is read, the user can first visually simulate the printing process. For finite element analysis, a part is voxelized to create discrete finite elements. Voxels are gradually included in the model to simulate the newly added line segment as per the g-code. The simulator requires clay properties such as density, initial moisture content, diffusion coefficient, simulation time and number of simulation steps. Assembly-free finite element solver [25] is used for faster computation to predict moisture content in the part during printing as well as passive drying.

The general schematic of the simulation process is shown in Figure 4. The g-code for the part printing is generated in standard slicing software incorporating the print orientation, layer height, wall thickness, infill density and print speed. Based on the user defined simulation time and print steps, moisture within the part as a function time (during printing and post-printing) can be simulated in the CPS. The accuracy is mesh-dependent. The moisture at the predefined locations, at user defined locations, are displayed.

Experiments

Two relatively simple, hollow cylinder, models were chosen to validate the proposed simulator. The hollow cylinders were 100mm tall, 100mm outer diameter, and varying thickness. One of the cylinders had two walls, while the other had four walls of thickness 4mm each as seen in Figure 5. Three equally spaced locations namely, A, B, and C are marked along the height of cylinders on both of these models for data collection. The g-code

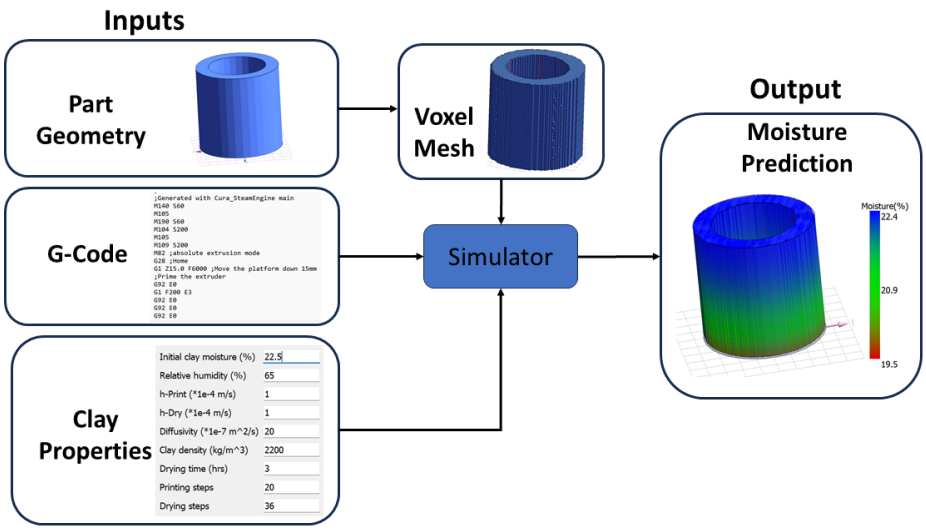

Figure 4: *Overview of Clay Printing Simulator (CPS).*

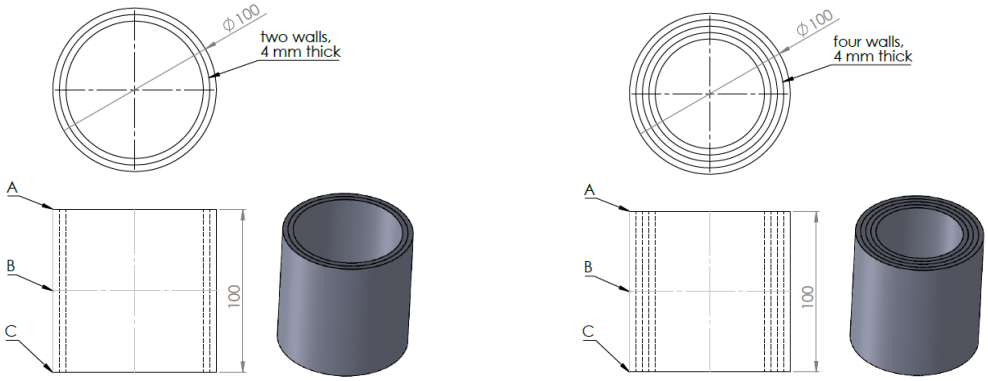

(a) *2-walled cylinder model* (b) *4-walled cylinder model*

Figure 5: *Hollow cylindrical specimens for experiments.*

for the models is generated using Cura®, with a layer height of 4mm and no infills. The simulator displays number of lines to print, and the amount of time it takes to print as shown in Figure 6.

The cylinders were meshed with 50000 voxel elements. Mesh convergence studies with different size meshes were carried out to ensure the reliability of results. For the boundary conditions, very high moisture absorption rates were imposed at the build plate interface.

Representative values of material and print parameters used for the experiments are provided in Table 1. Results for printing simulation at the start and end of print for a 4-walled hollow cylinder, are shown in Figure 7. The color bar shows moisture distribution on the part. The simulator also provides moisture values at every location within a part while printing, which is impossible to measure through physical experimentation. Change in moisture values at these locations until 2 hours of passive drying post printing are plotted in Figure 8.

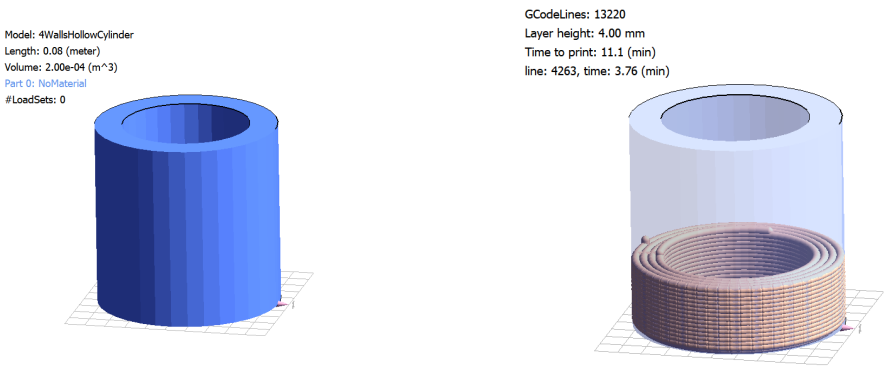

(a) *3D model loaded in CPS*

(b) *g-code simulation for wall printing*

Figure 6: *Inputs loaded into CPS for a 4-walled cylinder print simulation.*

Parameters	Value	Units
Dry Clay Modulus of Elasticity	0.6	MPa
Dry Clay Density	5	kg/m^3
Clay Diffusivity	0.9e-7	m^2/s
Initial Clay Moisture	22.5	%
Relative Humidity	65	%
Print Speed	5	mm/s
Proportionality Constant (β)	0.25	-
Number of print steps	50	-

Table 1: *Material and Print Parameters.*

(a) *Start of print*

(b) *End of print*

Figure 7: *Moisture simulation at different stages of clay 3D printing*

Validation

Two sets of the cylinders, for each wall thickness, were printed using a clay 3D printer. Average values of moisture across the specimens were recorded at the predefined locations A, B and C, at different intervals of time using standard moisture measurement procedure.

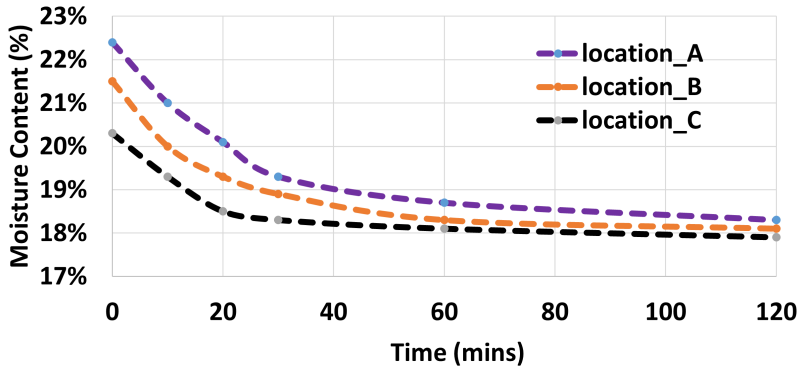

(a) *Moisture variation in 2-walled cylinder*

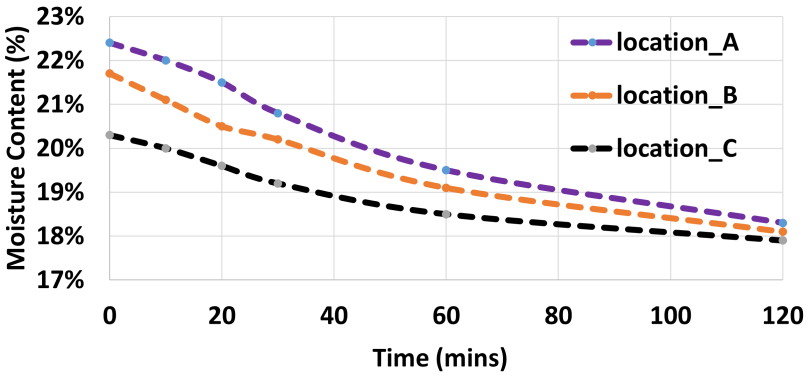

(b) *Moisture variation in 4-walled cylinder*

Figure 8: *Moisture variation predicted using CPS.*

Printed samples and experimental setups are shown in Figure 9. Samples were cut at the defined locations of the printed cylinders and weighted before and after drying to measure the moisture content. Results for moisture variation at different locations for the two sets

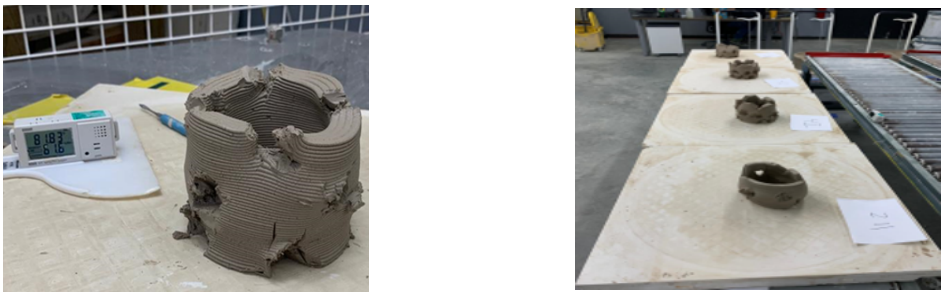

(a) (b)

Figure 9: *Experimental setup for moisture measurement*

of specimens are plotted against time and presented in Figure 10.

The measurements were taken after the part was fully printed so the plots show variation of moisture in the part during passive drying. Percentage values for obtained from physical experimental measurements are plotted as dotted lines for the three different locations in

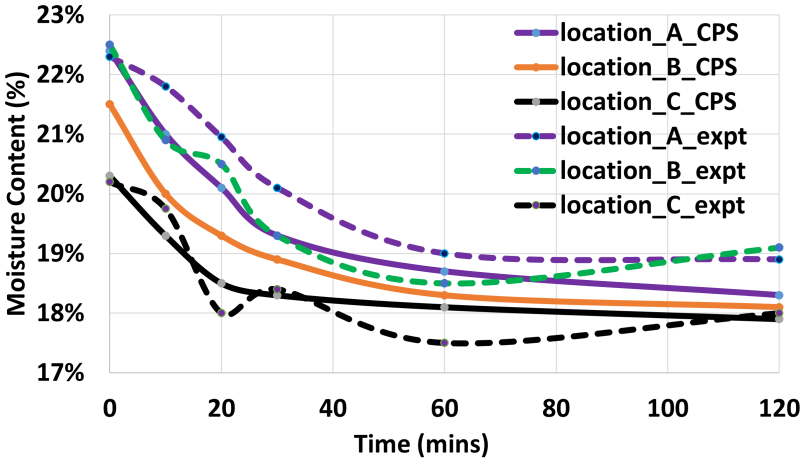

(a) *Moisture variation in 2-walled cylinder*

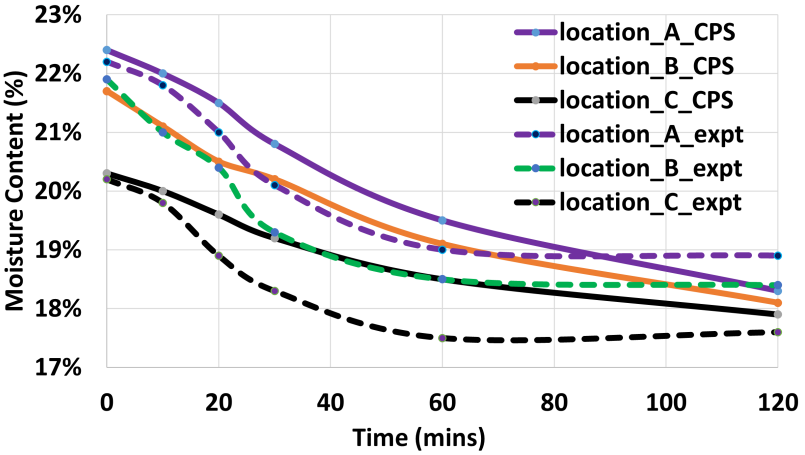

(b) *Moisture variation in 4-walled cylinder*

Figure 10: *Moisture variation comparison between CPS and experimental measurement.*

Figure 10, for both 2-walled and 4-walled cylinder specimens.

The plots indicate similar trends for change in moisture at different locations in the cylinders for data measured through physical experiments and numerical simulation in CPS. Small variation between experimental and numerical simulation results could be due to inherent errors such as change in room temperature, accuracy of tools etc, during physical measurements. Also linearity assumption for material properties in the simulation could be a source of error. Some noticeable deviation in moisture variation from experimental measurement for 2-walled cylinders can be seen in the plots. This could possibly be due to small feature sizes on the specimens. It took a lot of iterations to print these 2-walled cylinders as they have very thin walls that easily collapse during printing. The following assumptions have been made in the numerical model and in simulation, which could be the sources of error in these results.

- Material properties are considered to be constant and the part is assumed to be isotropic throughout the process.

- Material flow through the extruder is assumed to be consistent throughout the print process.
- No variation in the ambient temperature, relative humidity and air-flow has been assumed.

Some examples demonstrating the capability of CPS are shown in Figure 11. These parts

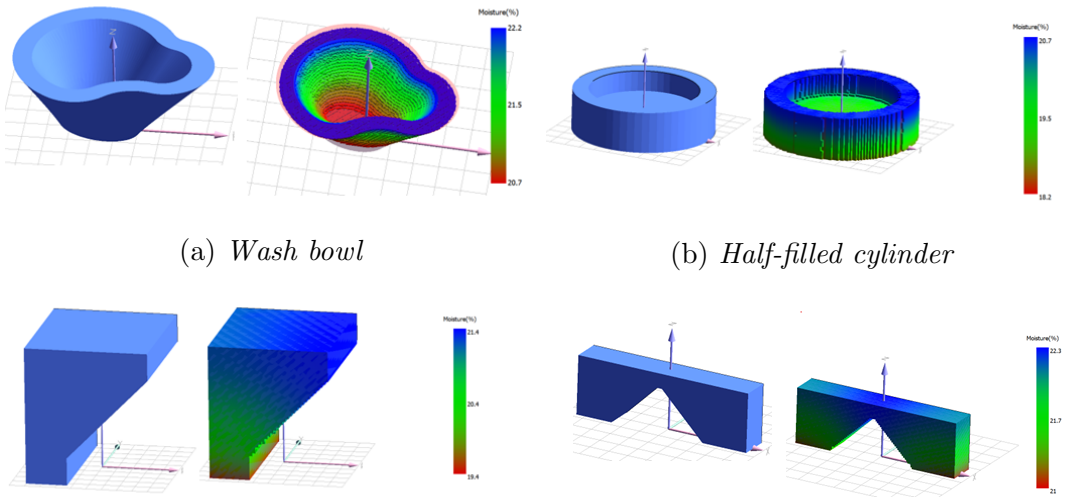

(a) *Wash bowl* (b) *Half-filled cylinder*

(c) *Wedge* (d) *Bridge design*

Figure 11: *Examples of moisture simulation on parts with different geometric features.*

with varying geometric features such as overhangs, infills, curved surfaces, sharp edges etc can be simulated to determine the moisture contents during printing as well as post printing.

Conclusion

A simulation tool was build to predict moisture in clay additive manufacturing. To the best of the author's knowledge, it is one of the first one of its kind. The simulator uses a CAD model, g-code and material properties for clay, to simulate the amount of moisture at any location in a part being printed. This tool allows for simulating the moisture distribution during printing as well as during passive drying post-printing for parts with varied geometric features and complexities. The simulator was validated using experimental results for moisture content on carefully choosen specimens at different locations and times within a part.

Future work will attempt to minimize these sources of error in between numerical and experimental results, for better accuracy and reliability of the tool. In addition, some of the possible extensions are listed below,

- More controlled physical experiments to validate parts with different geometric features will be carried out.

- A co-relation between drying and different modes of failures needs to be established to qualitatively predict chances of failures in clay 3D printing. This will require a large number of physical experiments with varied geometric, printing and material parameters.
- Effect of gravity and forced drying needs to be incorporated to better approximate actual printing process.

Acknowledgement

Physical experiments were performed by the members of Kohler Co. The authors would like to thank the team for their collaboration and also Kohler Co. for the generous support to conduct this research.

References

[1] Hui Chen, Liang Guo, Wenbo Zhu, and Chunlai Li. Recent advances in multi-material 3d printing of functional ceramic devices. *Polymers*, 14(21):4635, 2022.

[2] Yozi Ichida. Current status of 3d printer use among automotive suppliers: can 3d printed-parts replace cast parts. *IFEAMA SPSCP*, 5:69–82, 2016.

[3] Andrew Fox, Stephen Lynch, Jason C Young, Carl P Frick, Jennifer Hankins, Kyle Kuhn, Stephan A Brinckmann, and Ray S Fertig. Design and cooling performance of additively manufactured ceramic turbine vanes. *Journal of Turbomachinery*, 146(6), 2024.

[4] Qun Diao, Yong Zeng, and Jimin Chen. The applications and latest progress of ceramic 3d printing. *Additive Manufacturing Frontiers*, 3(1):200113, 2024.

[5] Chong Wang, Wei Huang, Yu Zhou, Libing He, Zhi He, Ziling Chen, Xiao He, Shuo Tian, Jiaming Liao, Bingheng Lu, et al. 3d printing of bone tissue engineering scaffolds. *Bioactive materials*, 5(1):82–91, 2020.

[6] Murat Bengisu and M Bengisu. *Engineering ceramics*, volume 620. Springer, 2001.

[7] Zhangwei Chen, Ziyong Li, Junjie Li, Chengbo Liu, Changshi Lao, Yuelong Fu, Changyong Liu, Yang Li, Pei Wang, and Yi He. 3d printing of ceramics: A review. *Journal of the European Ceramic Society*, 39(4):661–687, 2019.

[8] Xiaochen Sun, Maciej Mazur, and Chi-Tsun Cheng. A review of void reduction strategies in material extrusion-based additive manufacturing. *Additive Manufacturing*, 67:103463, 2023.

[9] Michael C Connelly. The drying of clay based ceramics. 9. 2003.

[10] Arslan Yousaf, Ans Al Rashid, and Muammer Koç. Parameter tuning for sustainable 3d printing (3dp) of clay structures. *Journal of Engineering Research*, 2024.

[11] Odysseas Kontovourkis and George Tryfonos. Robotic 3d clay printing of prefabricated non-conventional wall components based on a parametric-integrated design. *Automation in Construction*, 110:103005, 2020.

[12] Ala Abu Taqa, Mohamed O Mohsen, Mervat O Aburumman, Khalid Naji, Ramzi Taha, and Ahmed Senouci. Nano-fly ash and clay for 3d-printing concrete buildings: A fundamental study of rheological, mechanical and microstructural properties. *Journal of Building Engineering*, page 109718, 2024.

[13] Ofer Asaf, Arnon Bentur, Pavel Larianovsky, and Aaron Sprecher. From soil to printed structures: A systematic approach to designing clay-based materials for 3d printing in construction and architecture. *Construction and Building Materials*, 408:133783, 2023.

[14] Yazeed A Al-Noaimat, Mehdi Chougan, Mazen J Al-kheetan, Othman Al-Mandhari, Waleed Al-Saidi, Marwan Al-Maqbali, Haitham Al-Hosni, and Seyed Hamidreza Ghaffar. 3d printing of limestone-calcined clay cement: A review of its potential implementation in the construction industry. *Results in Engineering*, page 101115, 2023.

[15] Gieljan Vantyghem, Ticho Ooms, and Wouter De Corte. Fem modelling techniques for simulation of 3d concrete printing. *arXiv preprint arXiv:2009.06907*, 2020.

[16] Ticho Ooms, Gieljan Vantyghem, Ruben Van Coile, and Wouter De Corte. A parametric modelling strategy for the numerical simulation of 3d concrete printing with complex geometries. *Additive Manufacturing*, 38:101743, 2021.

[17] Shoukat Alim Khan, Hüseyin Ilcan, Ramsha Imran, Ehsan Aminipour, Oğuzhan Şahin, Ans Al Rashid, Mustafa Şahmaran, and Muammer Koç. The impact of nozzle diameter and printing speed on geopolymer-based 3d-printed concrete structures: Numerical modeling and experimental validation. *Results in Engineering*, 21:101864, 2024.

[18] RJM Wolfs and ASJ Suiker. Structural failure during extrusion-based 3d printing processes. *The International Journal of Advanced Manufacturing Technology*, 104:565–584, 2019.

[19] Dong An, YX Zhang, and Richard Chunhui Yang. Numerical modelling of 3d concrete printing: material models, boundary conditions and failure identification. *Engineering Structures*, 299:117104, 2024.

[20] Clayon. *Intuitive and professional modeling for ceramic 3D printing*, 2024. https://www.clayontec.com/en/.

[21] WASPCLAY. *Ceramic 3D printing*, 2024. https://www.3dwasp.com/en/ceramic-3d-printing-wasp-clay/.

[22] 3DCERAM. *3D Printing Software with Simplified Efficiency*, 2024. https://3dceram.com/3d-printing-softwares/.

[23] VoxelPrint and CobraPrint.

[24] JR Lowney and RD Larrabee. The use of fick's law in modeling diffusion processes. *IEEE Transactions on Electron Devices*, 27(9):1795–1798, 1980.

[25] Praveen Yadav and Krishnan Suresh. Large scale finite element analysis via assembly-free deflated conjugate gradient. *Journal of Computing and Information Science in Engineering*, 14(4):041008, 2014.